LA-UR -86-926 CONF-8604147--8

Received by OSTI

APR 07 1986

LA-UR--86-926

DE86 008735

TITLE: RAILGUNS POWERED BY EXPLOSIVE DRIVEN FLUX COMPRESSION GENERATORS

MASTER

AUTHOR(S): C. M. Fowler, E. L. Zimmermann, C. E. Cummings, R. F. Davidson, E. Foley, R. S. Hawke, J. F. Kerrisk, J. V. Parker, W. M. Parsons, D. R. Peterson, N. M. Schnurr, P. M. Stanley

SUBMITTED TO: the 3rd Symposium on Electromagnetic Launch Technology for publication.

DISCLAIMER

Los Alamos Los Alamos National Laboratory
Los Alamos, New Mexico 87545

FORM NO 836 R4
ST NO 2629 5/81

DISTRIBUTION OF THIS DOCUMENT IS UNLIMITED

RAILGUNS POWERED BY EXPLOSIVE DRIVEN FLUX COMPRESSION GENERATORS

C. M. Fowler, E. L. Zimmermann, C. E. Cummings, R. F. Davidson,
E. Foley, R. S. Hawke**, J. F. Kerrisk, J. V. Parker, W. M. Parsons,
D. R. Peterson***, N. M. Schnurr, and P. M. Stanley

Abstract - Explosive driven flux compression generators (FCG's) are single-shot devices that convert part of the energy of high explosives into electromagnetic energy. Some classes of these generators have served quite well as railgun power sources. In this paper and the following paper we describe strip and helical type FCG's, both of which are in use in the Los Alamos railgun program. Advantages and disadvantages these generators have for railgun power supplies will be discussed, together with experimental results obtained and some of the diagnostics we have found particularly useful.

INTRODUCTION

In most of the present U. S. railgun programs, prime energy is supplied by homopolar generators or capacitor banks. Often the energy is first delivered to an inductive storage unit to which the rails are either attached, or switched in later. In this and the following paper we survey that part of the Los Alamos program, much of which was done jointly with Lawrence Livermore National Laboratory, in which explosive-driven flux compression generators (FCG's) serve as the prime power source. The next section is devoted to a brief discussion of FCG's with emphasis on the two types we have found particularly useful - the strip generator and the helical generator. Some of the advantages and disadvantages of these power supplies are noted. A few of the diagnostics found to be particularly useful are then discussed. Included here are some measurements of plasma arc resistance for a large bore gun. Following this discussion, results of a single experiment are cited in which we believe it probable that a small tantalum projectile was accelerated to a velocity of order 10 km/sec. The limited diagnostic evidence available, together with the best modeling we can make in a reasonable way, are presented to the reader, whose conclusions are left to his own judgement. The major points of the paper are summarized in the final section.

FLUX COMPRESSION GENERATORS

Elements of FCG Operation

Explosive driven flux compression generators are single-shot devices that convert part of the energy of explosives into electromagnetic energy. Generally speaking, the devices consist of a conducting cavity containing magnetic flux in which part or all of the conductors are overlaid with explosive. Upon explosive detonation, the moving conductors work against the flux, thus imparting magnetic energy to the system. From a lumped parameter viewpoint, the process may be viewed as one in which the circuit inductance is forcibly reduced. In Fig. 1, the variable inductor L(t) represents the FCG, L_1 a load to be energized and I the current flowing in the system (I_0 and L_0 are initial current and generator inductance).

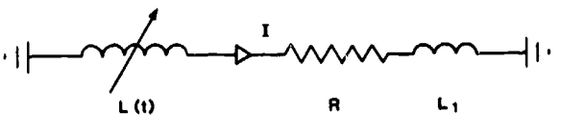

Fig. 1. Circuit schematics for load L_1 powered by flux compression generator L(t).

The system resistance is given by R. The corresponding circuit equation is

$$\frac{d}{dt}(L(t) + L_1)I + IR = 0 \quad . \tag{1}$$

If there was no circuit resistance, (all the cavity bounding elements were perfect conductors), then circuit flux would be conserved, or

$$\Phi_0 = (L(t) + L_1)I = (L_0 + L_1)I_0 \tag{2}$$

At generator burnout, where the generator inductance has been reduced to zero, the final load current and energy, $L_1I^2/2$ are increased by a factor $(L_0+L_1)/L_1$, or

$$I/I_0 = E/E_0 = (L_0 + L_1)/L_1 \tag{3}$$

As seen from (1), circuit resistive elements lead to a loss of flux with a consequent reduction of both current and energy.

Strip and Helical FCG's

FCG's are constructed in a variety of types, depending upon the load requirements. We discuss here the two types we have used to power railguns, the strip and the helical generator. A more general introductory discussion of these devices, together with a rather comprehensive lumped circuit analysis, are available in [1]. The strip generator shown schematically on Fig. 2 has been used most often as a railgun power source at Los Alamos. Typically, the generator consists of long parallel strips of copper, one of which is overlaid with explosive strips; an input block for leads from a capacitor bank that

The authors are with the Los Alamos National Laboratory, Los Alamos, NM, 87545 and
**Lawrence Livermore National Laboratory, Livermore, CA, 94550 and
***The University of Texas, Center for Electromechanics, Austin, TX, 78758.

This work was supported by the U.S. Department of Energy, the Ballistic Missile Defense Advanced Technology Center and the Defense Advanced Research Projects Agency.

supplies the initial flux to the system; and an output block for connections to the load. In the present situation, the load consists of the railgun, occasionally preceded by a ballast storage inductor. In one such generator, the copper strips are 2.4 m long, 57 mm wide, and 1.6 mm thick, and the separation between them is 51 mm. Two layers of C-8 Detasheet explosive, 51 mm wide, are placed over the upper copper strip. To minimize expansion of generator components from magnetic forces, steel ballast bars, 50.8 mm wide by 12.7 mm to 25.4 mm thick, are laid on top of the Detasheet explosive and directly under the bottom copper strip. The wedge-shaped input and output blocks are cut from 50.8 mm square brass bar stock and then drilled and tapped individually to accommodate cable input header attachments and to make output connections to the various loads tested.

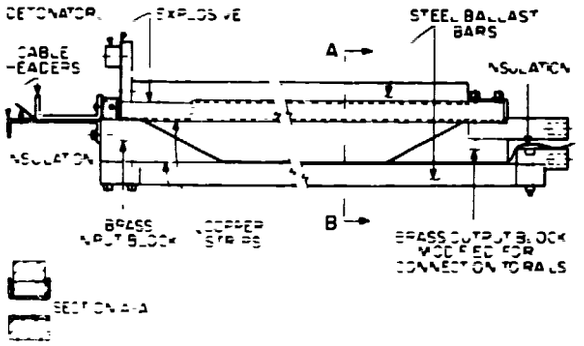

Fig. 2. Strip generator components.

After flux from a capacitor bank is introduced into the generator and the load, the detonator is fired. The input slot is closed to trap the flux, and detonation proceeds down the Detasheet strips. When the top plate is driven into the bottom plate, it pushes the flux into the load. Nearly all of the dimensions have been varied to meet different conditions. Copper strip lengths have ranged from 1 to 3.6 meters, widths from 50.8 to 102 mm and thicknesses from 1.6 to 3.2 mm, with corresponding changes in the input and output block dimensions, and in the thickness and width of the explosive layers.

Figure 3a shows the basic components of a helical type generator. At the lower right is an external load coil which is to be energized by the generator. The generator itself consists of an external helical winding, an explosive-loaded metal cylinder, or armature, and input and output insulating spacers to center the armature in the helix. Initial flux is supplied to the generator and series load coil from a capacitor bank. It can be seen that the armature itself serves as part of the conducting circuit. When the explosive is detonated, the armature expands, resulting in a conical metal front moving with explosive detonation velocity. The detonation is so timed that this conical front shorts out the generator input at or near peak current or, equivalently, peak flux in the generator. This also effectively isolates the capacitor bank from the system. After closure of the current input, the conical front proceeds down the armature, contacting the helical turns in a more or less wiping fashion. Figure 3b gives a view of the generator fairly late in the detonation stage.

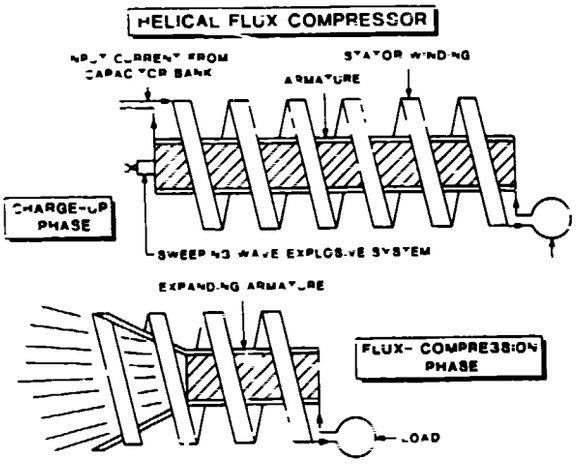

Fig. 3(a). Elements of a helical flux compression generator used to power a load L_1. The central tube, or armature is loaded with (b). View of the generator some time after the explosive has been detonated.

The inductance of the generator is roughly proportional to the square of the number of turns in the helix, and inversely proportional to the length over which the turns are spaced. Because of the multiple turns, these generators usually have much larger initial inductances than those of other classes. As seen from (3), they generally have much higher gain capability than that of other generator types. Since currents normally increase during generator turn time, the conductors are normally widened towards the generator output to accommodate the larger currents. Unlike strip generators, it is difficult and expensive to build these generators with burn times longer than two or three hundred microseconds. Consequently, we have used these generators to energize an inductive store to which the railgun is attached, instead of driving the railgun directly, as is frequently the case with the strip generators. Design details of this generator are given in the following companion paper [2] as well as its application to accelerate massive projectiles.

Advantages and Disadvantages of FCG's

The most obvious disadvantage of FCG's is the use of explosives with their consequent hazards and destruction of generator components. Another factor is that their performance is usually better when they operate in a high energy density environment. Thus, it becomes inconvenient (and expensive) to use them in low level test series that require many shots. On the other hand, we have found them very useful when operated at high current levels. We have fired as many as four such shots in a day. The limiting factor has not been the replacement of the FCG's so much as the time required to refurbish or replace the railguns themselves, since they usually suffer significant damage from carrying large currents. The railguns are, of course, protected from any direct explosive damage.

Among the advantages of FCG's are portability and versatility. As an example of portability, in a series of experiments, FCG's were used as rocket-borne plasma gun power supplies, requiring weights and volumes of only a few percent of those in more

conventional supplies [3]. They could also prove useful in remote locations where it might be impractical to mount conventional supplies. Within limits, generators can be designed to meet various required test conditions. The strip generator, for example, can be easily modified in a number of ways [4]. These include easy adjustment of conductor lengths for pulse length control, altering the conductor widths along the generator to meet varying current requirements, changing the inter-conductor distance and, within limits, varying the spacing as well as the conductor widths to vary the inductance gradient along the generator. Various combinations of more than one generator can be used. By adding a third, isolated, element to the railgun breech connections, two generators have been fired in parallel, but remain series connected, as seen in Fig. 4. This results in doubling the generator inductance without increasing the burnout time. On the other hand by simply connecting the generators in series and firing sequentially, both the generator inductance and pulse length would be doubled. Peterson [5] has also pointed out some of the advantages of phase firing several generators connected at different stations in long railguns.

Fig. 4. Photograph showing two strip generators series connected to a railgun. In this shot the generators were fired in parallel. Seen at the lower left are a witness plate in front of the gun and a 2.2 m long x-ray film cassette.

More than most power sources, the effectiveness of FCG's relies to a considerable extent on minimizing flux losses, as can be seen from (3). Among the losses are penetration of flux into the skin of metal conductors and pocketing of flux. This latter loss occurs when the moving conductors close off part of the circuit prematurely, thus isolating this part of the flux from the useful part of the system. Bichenkov [6] discusses these losses in some detail. Normally, FCG conductors are thick compared to skin-depth penetration distances. However, for hydrodynamic reasons, moving strip generator conductors are relatively thin - a few millimeters or less. Additional losses can occur by flux leaking through these conductors, for sufficiently long pulses, such as those required for some railgun applications [7].

For plasma arc driven railguns, the arc resistance leads to flux losses. According to (1), this is given by the time integral of the arc voltage. As an example of the magnitude of this loss, consider a strip generator of initial inductance 1.5 uH, loaded by a current of 0.67 MA. These are typical values. The initial generator flux is 1.0 Webers. If the plasma arc voltage were 500 V, 25% of the initial flux would be lost in 500 us. As a means of reducing this loss, solid armatures might be better, particularly when accelerating large masses to moderate velocities.

USEFUL DIAGNOSTICS

Some of the diagnostics we have found particularly useful are described in this section. These include plasma armature voltage, magnetic probes for monitoring both current and position of the projectile in the gun, and flash x-ray diagnostics.

Plasma Armature Voltage

The HIMASS tests, treated in detail in the following companion paper [2], are excellent examples of the utility of FCG's in obtaining preliminary experimental results without a large investment in specialized equipment and facilities. One of the important issues addressed in the HIMASS tests is the scaling of plasma armature voltage with bore diameter.

The plasma armature voltage is an important parameter in the design of future large bore launchers because it directly determines the power dissipation in the bore and, indirectly, such factors as system efficiency and wall ablation. Scaling to large diameter has generally required extrapolation using the large data base for bore diameters less than 2 cm. This extrapolation is unreliable because electrode and material effects play an important, and generally unquantified, role for small bore diameter.

Plasma armature voltage was measured during the HIMASS tests by connecting a 94 Ω resistor across the rails at the muzzle. The current through this resistor was measured with a current transformer (Pearson model 411) to ensure isolation of the measuring apparatus from the railgun. The current transformer was shielded with 5.4 mm of iron to prevent false signals from the strong ambient magnetic fields.

The recorded voltage waveform is shown in Fig. 5. The input current waveform is also shown for reference. The following features are noteworthy.

The high voltage spike at 95 us is generated by the vaporization of the aluminum foil fuse. Plasma measurements begin only after the voltage returns to a steady value.

The large double spike at about 600 us is generated by variations in dI/dt caused by the FCG coil structure. This feature can be removed using the recorded dI/dt waveform and adjusting the plasma armature inductance to eliminate the double peak structure. The best correction is obtained for a fuse inductance of 40 nH, a reasonable value for this plasma-rail geometry. The corrected voltage waveform is shown by the dashed line in Fig. 5.

There are three distinct phases of operation illustrated in Fig. 5. The first phase extends from 0 to 430 us. Here the current waveform is a quarter cycle sinusoid with a peak current of 160 kA. The current per unit railgun width is small (2 kA/mm) and the plasma resistance is high (~10 mΩ). Both the power and energy input are small, approximately 100 kW/cc and 30 J/cc respectively.

During the second phase from 430 to 630 us the current rises rapidly to a peak of 2.5 MA. The power input and energy input rise dramatically and the plasma becomes highly ionized. The peak power reaches

3.7 MW/cc and the energy input to the plasma reaches 280 J/cc. During this phase the resistance drops rapidly to 0.5 mΩ.

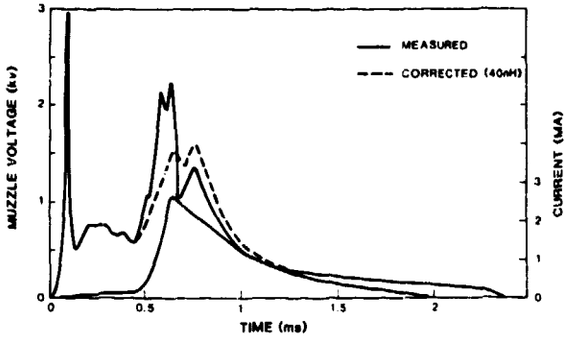

Fig. 5. Solid curves show measured muzzle voltage and current from a 102 mm bore railgun shot. The corrected muzzle voltage is shown by dashed lines.

The final phase extends from peak current to the end of current flow. During this period the plasma resistance is nearly constant at 0.5 mΩ even though substantial power and energy continue to be dissipated in the plasma. Only at late times when the current has fallen below 10% of its peak value does the plasma resistance begin to rise.

This behavior suggests that the ionization level in the plasma adjusts very rapidly (10's of microseconds) to increasing current but only slowly as the current decreases. Since equilibrium ionization is reached rapidly we believe that the voltage measured at and shortly after peak current is representative of the operating voltage at 2.6 MA despite the fact that this is far from a steady state measurement.

Magnetic Probes

An array of magnetic pickup probes spaced along the railgun barrel is routinely employed in all tests. Depending upon position and orientation various information concerning the projectile and plasma armature may be derived from these probes. A typical application is illustrated in Fig. 1 of Ref. [2] for a recent HIMASS test. In this case, the probes are positioned on the outside surface of the barrel. Frequently, however, they are placed in recessed holes drilled in the barrel to bring them closer to the rails. Typically the probe pickup coils consist of 10 turns of #28 copper wire, wound closely on a 12 mm diameter form.

The output from each coil is integrated with a passive integrator and recorded on an oscilloscope. Usually 5 ms integrator time constants are sufficient. To provide quantitative data the entire array is calibrated prior to the test by shorting the muzzle and discharging a capacitor bank through the gun at a low current (100 kA). The calibration waveforms show that the coils have a time dependent response due to current diffusion into the rails. For qualitative interpretation this time dependence can be neglected. For quantitative measurements an algorithm has been developed to remove the time-dependent effects. For the HIMASS shot described in Ref. [2], the probes had a measured response of 0.25 V/MA at early time falling to 0.16 V/MA at late time.

The probe signals are quite useful. When no current breakdowns occur between the current source and the projectile, the probe signals ultimately scale with the railgun input current. This scaling occurs after a finite pulse risetime starting at the time the projectile passes the probe station. The risetime length allows a qualitative estimate of the length of the plasma armature. When current breakdowns do occur, as happened on other shots, the probe signals from stations corresponding to positions reached by the projectile after breakdown show lack of scaling with the input current signal. These signals allow at least an approximate calculation of the actual plasma arc current, which might be substantially less than the total input current.

Flash X-Ray Diagnostics

Two flash x-rays (Hewlett-Packard, equivalent Model 43733A, 300 kV at remote heads) are normally used on every shot to photograph the projectile after it leaves the gun. Since the heads are fired at different preset times, the film images allow calculation of the projectile velocity in air. Figure 4 of Ref. [2] is a good example of such a record. From this film it was determined that the 600 g lexan projectile reached a velocity of 1.0 km/s. The beams are sufficiently intense that they can film reliably over projectile travel distances greater than four meters. The cassettes are loaded with a double layer of film and sandwiched between image enhancement screens. Occasionally imperfections are noticed on the films, probably arising from our development process. The use of double films, developed separately, allows identification of such flaws. The two x-ray heads are positioned in such a way that the projectile shadowgraphs appear at different vertical heights on the film. Thus, the vertical location of the projectile image on the film plane identifies the particular x-ray head responsible for the image, and the time (preset) at which it was taken.

Fig. 6. Lower view: x-ray photograph of compound projectile in free flight. The steel ball was originally at the front of the lexan sabot. Upper view: x-ray photograph taken shortly after projectile struck a steel witness plate.

Such time identiffcation is unnecessary when both images are observed, but is invaluable when one of the images is missed, a not infrequent occurrence. Although our other diagnostics have substantially improved, when there is disagreement between them, the flash x-ray diagnostics serve as the final court of appeals.

Frequently, the x-ray images reveal unexpected information, such as shown in Fig. 6. The lower view shows a projectile in free flight consisting of a steel ball embedded in lexan. Interestingly, the steel ball was cast near the front face of the projectile. During acceleration, the lexan moved around the heavy steel ball. The upper view, taken later in time, shows spallation of a steel witness plate after being struck by the projectile.

HIGH VELOCITY SHOT

On November 24, 1981, Lawrence Livermore and Los Alamos people collaborated on a railgun shot in which it was thought that the projectile reached a velocity of 11±1 km/s. The railgun overall length was 4.9 m. The cylindrical projectile consisted of a thin tantalum disc housed in a lexan sabot, total weight 2.8 g. A strip generator was used as the power supply. The entire gun was housed in a large diameter pipe, which was evacuated. A number of different railgun shots were fired in this series. With the rather tight firing schedule, two shots were originally planned for the 4.9 m gun. In all, however, the test series was extended so that four shots were fired with this gun. In the first three shots, electrical breakdown occurred at the breech, owing to our inability to achieve a good vacuum.

For the last test, the large pipe was removed and the shot was fired in air. Owing to ambiguous signals from other diagnostics, the only useful data obtained for this shot were the current record and a single flash x-ray picture. The x-ray image showed only the tantalum disc, the sabot presumably having been stripped away. We have never photographed a whole plastic projectile moving in air faster than about 5.5 km/s, and even then the original cubical projectile had assumed a mushroom shape [8]. The projectile traveled 4.7 m in the gun and traveled an additional 4.0 m in air at the time the x-ray was triggered, 1130 μs after the start of current flow in the gun. Several simple velocity calculations were made. Assuming constant acceleration in the gun, a velocity of 11.9 km/s is obtained. From the integral of the current squared, with no losses, velocities in the range of 10-12 km/s were obtained, using some small variations for dL/dx and making some allowance for the air mass contained in the gun, (~0.4 g). A lower bound of 7.7 km/s is obtained if it is assumed that the entire velocity arose from a single impact at time zero, not a realistic hypothesis.

At the time, it was thought reasonable to ascribe a velocity of 11±1 km/sec, but the result has not been widely cited, owing to the incompleteness of the diagnostics. Since that time, much more sophisticated railgun codes have been developed, such as the Los Alamos Railgun Estimator (LARGE) code [9], which has been used to simulate the performance of the experiment.

The LARGE code can model various kinds of power supplies, explosively-driven magnetic flux compression generators, and rail configurations. An attempt was made in writing LARGE to use as few empirical models or parameters as possible within the constraints of a fast running code. To this extent, all rail inductances and resistances are calculated from a physical description of the rails. A calculated rail inductance gradient (high-frequency limit) is used to determine the force on the projectile [10]. Estimates of how current diffusion changes rail inductance with time are also included [11].

The code has been recently refined to include the analysis of rail and insulator material ablation and its effect on railgun performance [12]. A thermal analysis is used to estimate the ablation rate and all the material ablated is assumed to be ionized and entrained in the arc. Viscous drag on the arc is calculated and included in the force calculations.

Results of the simulation of the 11/24/81 experiment are shown in Figs. 7 and 8. The velocity is predicted to reach a maximum value of 9.3 km/s approximately 1.0 m from the muzzle. This occurs when the drag force on the arc offsets the magnetic force that is decreasing as the current drops. The time required to reach the x-ray camera station located 4.0 m from the muzzle (assuming constant projectile velocity in free flight) is 1190 μs. This is 5.3% higher than the experimentally measured value of 1130 μs.

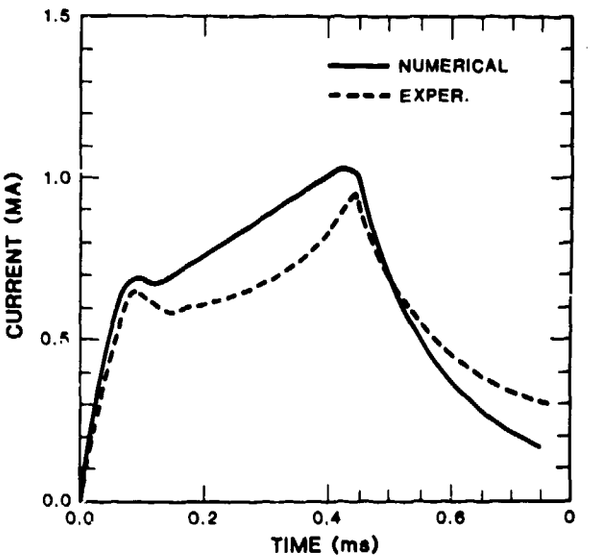

Fig. 7. Simulated and experimental current profiles for high velocity shot.

The currents used to compute the accelerating force are somewhat larger than the experimental values (see Fig. 7). The actual slope of the velocity vs time curve should therefore be slightly smaller than that shown in Fig. 8. The muzzle velocity would have to be significantly higher than the predicted value if the predicted elapsed time to the x-ray camera is to agree with the measured value. This indicates that the code somewhat overpredicts the effects of ablation and arc drag at high velocities. Although an exact determination of muzzle velocity cannot be made, the comparison of the simulation to the experimental results indicates a value of at least 10.0 km/s.

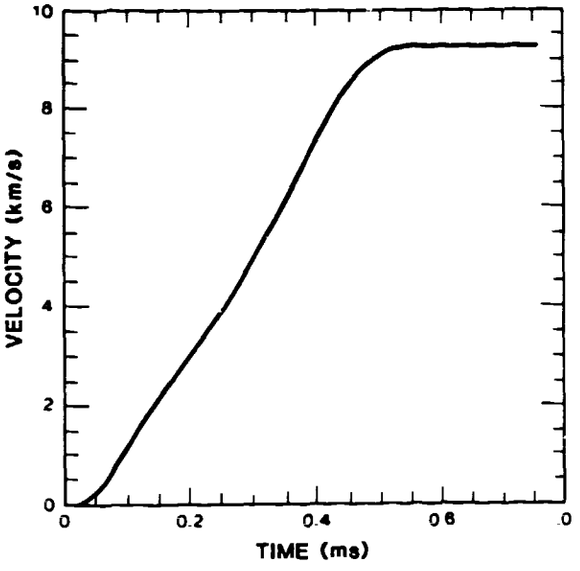

Fig. 8. Simulated projectile velocity profile for high velocity shot.

SUMMARY

In this paper, we give a brief overview of flux compression generators noting, in particular, strip and helical generators that have been used as railgun power sources. Advantages and disadvantages of the generators are pointed out. The need to minimize flux losses is emphasized.

Several types of diagnostics found to be particularly useful are discussed. These include muzzle voltage measurements, from which it was shown that the plasma arc resistance for a very large bore gun was consistent with that for small-bore guns; magnetic probes that monitor projectile position, detect alternate current breakdowns behind the projectile, and allow estimates of the plasma arc length; flash x-radiography from which projectile velocities and other useful information can be obtained.

Finally, a discussion is given of a shot in which a projectile is thought to have achieved a velocity of 10 km/s or greater. The incomplete experimental evidence led to a velocity estimated at 11±1 km/s. A recent, almost ab initio, calculation with a much more sophisticated code suggests a velocity of 10 km/s or greater. The authors have put all their cards on the table, so to speak. Acceptance of the result is, ultimately, left to the judgement of the reader.

REFERENCES

[1] C. M. Fowler, R. S. Caird, and W. B. Garn, "An Introduction to Explosive Magnetic Flux Compression Generators," Los Alamos National Laboratory report LA-5893-MS, March 1975.

[2] E. L. Zimmerman, C. M. Fowler, E. Foley, and J. V. Parker, "Himass Electromagnetic Launcher at Los Alamos," Paper presented at the conference.

[3] C. M. Fowler, D. B. Thomson, W. B. Garn, and R. S. Caird, "Los Alamos National Laboratory Group M-6 Summary Report, The Birdseed Program," Los Alamos National Laboratory report, LA-5141-MS, Jan. 1973.

[4] C. M. Fowler, D. R. Peterson, J. F. Kerrisk, R. S. Caird, D. J. Erickson, B. L. Freeman, and J. H. Goforth, "Explosive Flux-Compression Strip Generators," in Ultrahigh Magnetic Fields, V. M. Titov and G. A. Shvetsov, Eds. Moscow: Navka, 1984, pp. 282-291.

[5] D. R. Peterson, Center for Electromechanics, U of Texas, Austin, Private Communication.

[6] E. I. Bichenkov and V. A. Lobanov, "Limiting Currents and Losses in Unshaped Flat and Coaxial Magnetic Compression Generators," Plenum Publishing Corporation Translation, 1981, from Fizika Goreniya I Vzryva, Vol. 16, No. 5, pp. 40-47, Sep.-Oct. 1980.

[7] C. M. Fowler "Losses in Railgun Flux Compression Generators" Los Alamos National Laboratory report LA-UR 85-2555, Aug. 1985.

[8] R. S. Hawke, A. L. Brooks, F. J. Deadrick, J. K. Scudder, C. M. Fowler, R. S. Caird and, D. R. Peterson, "Results of Railgun Experiments Powered by Magnetic Flux Compression Generators," IEEE Trans. on Magn., Vol. MAG-18, No. 1, Jan. 1982, pp. 82-93, compare Figs. 9a and 9c.

[9] J. F. Kerrisk, "Electrical and Thermal Modeling of Railguns," IEEE Transactions on Magnetics, Vol. MAG-20, pp. 399-402, March 1984.

[10] J. F. Kerrisk, "Current Distribution and Inductance Calculation for Railgun Conductors," Los Alamos National Laboratory report LA-9092-MS, Oct. 1980.

[11] J. F. Kerrisk, "Current Diffusion in Railgun Conductors," Los Alamos National Laboratory report LA-9401-MS, June 1982.

[12] N. M. Schnurr and J. F. Kerrisk, "Numerical Studies of Ablation and Ionization of Railgun Materials," AIAA 18th Fluid Dynamics and Plasmadynamics and Laser Conference, July 16-18, 1985, Cincinnati, Ohio, AIAA-85-1576.